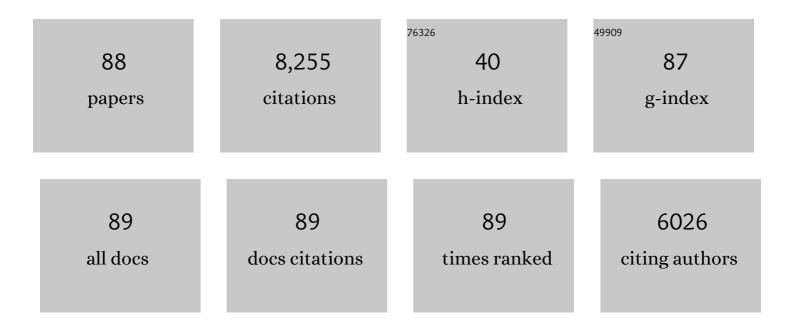
List of Publications by Year in descending order

Source: https://exaly.com/author-pdf/7305785/publications.pdf Version: 2024-02-01



**ΡΑΒΙ Ο ΒΕΛΤΟ** 

#	Article	IF	CITATIONS
1	Conversion of Methanol to Hydrocarbons: How Zeolite Cavity and Pore Size Controls Product Selectivity. Angewandte Chemie - International Edition, 2012, 51, 5810-5831.	13.8	1,476
2	A Consistent Reaction Scheme for the Selective Catalytic Reduction of Nitrogen Oxides with Ammonia. ACS Catalysis, 2015, 5, 2832-2845.	11.2	400
3	Magnetite Nanocrystals: Nonaqueous Synthesis, Characterization, and Solubilityâ€. Chemistry of Materials, 2005, 17, 3044-3049.	6.7	341
4	Revisiting the nature of Cu sites in the activated Cu-SSZ-13 catalyst for SCR reaction. Chemical Science, 2015, 6, 548-563.	7.4	341
5	Characterization of Cu-exchanged SSZ-13: a comparative FTIR, UV-Vis, and EPR study with Cu-ZSM-5 and Cu-β with similar Si/Al and Cu/Al ratios. Dalton Transactions, 2013, 42, 12741.	3.3	317
6	Methane to Methanol: Structure–Activity Relationships for Cu-CHA. Journal of the American Chemical Society, 2017, 139, 14961-14975.	13.7	277
7	Structure–deactivation relationship for ZSM-5 catalysts governed by framework defects. Journal of Catalysis, 2011, 280, 196-205.	6.2	265
8	Assessing the acid properties of desilicated ZSM-5 by FTIR using CO and 2,4,6-trimethylpyridine (collidine) as molecular probes. Applied Catalysis A: General, 2009, 356, 23-30.	4.3	249
9	Interaction of NH <sub>3</sub> with Cu-SSZ-13 Catalyst: A Complementary FTIR, XANES, and XES Study. Journal of Physical Chemistry Letters, 2014, 5, 1552-1559.	4.6	248
10	The Cu-CHA deNO <sub><i>x</i></sub> Catalyst in Action: Temperature-Dependent NH <sub>3</sub> -Assisted Selective Catalytic Reduction Monitored by Operando XAS and XES. Journal of the American Chemical Society, 2016, 138, 12025-12028.	13.7	243
11	Cu-CHA – a model system for applied selective redox catalysis. Chemical Society Reviews, 2018, 47, 8097-8133.	38.1	215
12	Shape Selectivity in the Conversion of Methanol to Hydrocarbons: The Catalytic Performance of One-Dimensional 10-Ring Zeolites: ZSM-22, ZSM-23, ZSM-48, and EU-1. ACS Catalysis, 2012, 2, 26-37.	11.2	207
13	The Nuclearity of the Active Site for Methane to Methanol Conversion in Cu-Mordenite: A Quantitative Assessment. Journal of the American Chemical Society, 2018, 140, 15270-15278.	13.7	177
14	Catalyst deactivation by coke formation in microporous and desilicated zeolite H-ZSM-5 during the conversion of methanol to hydrocarbons. Journal of Catalysis, 2013, 307, 62-73.	6.2	169
15	Composition-driven Cu-speciation and reducibility in Cu-CHA zeolite catalysts: a multivariate XAS/FTIR approach to complexity. Chemical Science, 2017, 8, 6836-6851.	7.4	163
16	Selectivity control through fundamental mechanistic insight in the conversion of methanol to hydrocarbons over zeolites. Microporous and Mesoporous Materials, 2010, 136, 33-41.	4.4	141
17	Conversion of methanol over 10-ring zeolites with differing volumes at channel intersections: comparison of TNU-9, IM-5, ZSM-11 and ZSM-5. Physical Chemistry Chemical Physics, 2011, 13, 2539-2549.	2.8	137
18	Methanol-to-hydrocarbons conversion: The alkene methylation pathway. Journal of Catalysis, 2014, 314, 159-169.	6.2	136

#	Article	IF	CITATIONS
19	Conversion of Methanol to Hydrocarbons: Spectroscopic Characterization of Carbonaceous Species Formed over H-ZSM-5. Journal of Physical Chemistry C, 2008, 112, 9710-9716.	3.1	127
20	Methylation of benzene by methanol: Single-site kinetics over H-ZSM-5 and H-beta zeolite catalysts. Journal of Catalysis, 2012, 292, 201-212.	6.2	126
21	High Zn/Al ratios enhance dehydrogenation vs hydrogen transfer reactions of Zn-ZSM-5 catalytic systems in methanol conversion to aromatics. Journal of Catalysis, 2018, 362, 146-163.	6.2	120
22	Synthesis and Characterization of Stable and Crystalline Ce1-xZrxO2 Nanoparticle Sols. Chemistry of Materials, 2004, 16, 2599-2604.	6.7	119
23	Synthesis of Yttria-Based Crystalline and Lamellar Nanostructures and their Formation Mechanism. Small, 2004, 1, 112-121.	10.0	118
24	New insights into catalyst deactivation and product distribution of zeolites in the methanol-to-hydrocarbons (MTH) reaction with methanol and dimethyl ether feeds. Catalysis Science and Technology, 2017, 7, 2700-2716.	4.1	106
25	How defects and crystal morphology control the effects of desilication. Catalysis Today, 2011, 168, 38-47.	4.4	103
26	Hydrogen Transfer versus Methylation: On the Genesis of Aromatics Formation in the Methanol-To-Hydrocarbons Reaction over H-ZSM-5. ACS Catalysis, 2017, 7, 5773-5780.	11.2	102
27	Structure–deactivation relationships in zeolites during the methanol–to-hydrocarbons reaction: Complementary assessments of the coke content. Journal of Catalysis, 2017, 351, 33-48.	6.2	82
28	Distribution of Aluminum over the Tetrahedral Sites in ZSM-5 Zeolites and Their Evolution after Steam Treatment. Journal of Physical Chemistry C, 2018, 122, 15595-15613.	3.1	82
29	A Straightforward Descriptor for the Deactivation of Zeolite Catalyst H-ZSM-5. ACS Catalysis, 2017, 7, 8235-8246.	11.2	77
30	Benzene co-reaction with methanol and dimethyl ether over zeolite and zeotype catalysts: Evidence of parallel reaction paths to toluene and diphenylmethane. Journal of Catalysis, 2017, 349, 136-148.	6.2	70
31	Kinetics of Zeolite Dealumination: Insights from H-SSZ-13. ACS Catalysis, 2015, 5, 7131-7139.	11.2	69
32	Morphology-induced shape selectivity in zeolite catalysis. Journal of Catalysis, 2015, 327, 22-32.	6.2	64
33	Probing the surface of nanosheet H-ZSM-5 with FTIR spectroscopy. Physical Chemistry Chemical Physics, 2013, 15, 13363.	2.8	53
34	Investigating the Low Temperature Formation of Cu <sup>II</sup> â€(N,O) Species on Cuâ€CHA Zeolites for the Selective Catalytic Reduction of NO <sub>x</sub> . Chemistry - A European Journal, 2018, 24, 12044-12053.	3.3	53
35	Analysis of structural transformations during the synthesis of a MoVTeNb mixed oxide catalyst. Applied Catalysis A: General, 2006, 307, 137-147.	4.3	52
36	Operando Raman spectroscopy applying novel fluidized bed micro-reactor technology. Catalysis Today, 2013, 205, 128-133.	4.4	45

#	Article	IF	CITATIONS
37	Zeolite Surface Methoxy Groups as Key Intermediates in the Stepwise Conversion of Methane to Methanol. ChemCatChem, 2019, 11, 5022-5026.	3.7	45
38	Nitrate–nitrite equilibrium in the reaction of NO with a Cu-CHA catalyst for NH <sub>3</sub> -SCR. Catalysis Science and Technology, 2016, 6, 8314-8324.	4.1	44
39	Synthesis of mesoporous ZSM-5 zeolite encapsulated in an ultrathin protective shell of silicalite-1 for MTH conversion. Microporous and Mesoporous Materials, 2020, 292, 109730.	4.4	44
40	Collective action of water molecules in zeolite dealumination. Catalysis Science and Technology, 2019, 9, 3721-3725.	4.1	43
41	Selective oxidation of propylene to acrolein by hydrothermally synthesized bismuth molybdates. Applied Catalysis A: General, 2014, 482, 145-156.	4.3	41
42	Time- and space-resolved study of the methanol to hydrocarbons (MTH) reaction – influence of zeolite topology on axial deactivation patterns. Faraday Discussions, 2017, 197, 421-446.	3.2	39
43	Bismuth Molybdate Catalysts Prepared by Mild Hydrothermal Synthesis: Influence of pH on the Selective Oxidation of Propylene. Catalysts, 2015, 5, 1554-1573.	3.5	38
44	EXAFS wavelet transform analysis of Cu-MOR zeolites for the direct methane to methanol conversion. Physical Chemistry Chemical Physics, 2020, 22, 18950-18963.	2.8	35
45	Unit cell thick nanosheets of zeolite H-ZSM-5: Structure and activity. Topics in Catalysis, 2013, 56, 558-566.	2.8	33
46	MoS2 supported on P25 titania: A model system for the activation of a HDS catalyst. Journal of Catalysis, 2015, 328, 225-235.	6.2	33
47	Deactivation of Zeolite Catalyst H-ZSM-5 during Conversion of Methanol to Gasoline: Operando Time- and Space-Resolved X-ray Diffraction. Journal of Physical Chemistry Letters, 2018, 9, 1324-1328.	4.6	33
48	Deactivation behavior of an iron-molybdate catalyst during selective oxidation of methanol to formaldehyde. Catalysis Science and Technology, 2018, 8, 4626-4637.	4.1	32
49	Conversion of methanol to hydrocarbons over zeolite ZSM-23 (MTT): exceptional effects of particle size on catalyst lifetime. Chemical Communications, 2017, 53, 6816-6819.	4.1	31
50	Role of internal coke for deactivation of ZSM-5 catalysts after low temperature removal of coke with NO2. Catalysis Science and Technology, 2012, 2, 1196.	4.1	30
51	Time- and space-resolved high energy operando X-ray diffraction for monitoring the methanol to hydrocarbons reaction over H-ZSM-22 zeolite catalyst in different conditions. Surface Science, 2016, 648, 141-149.	1.9	30
52	Understanding and Optimizing the Performance of Cuâ€FER for The Direct CH <sub>4</sub> to CH <sub>3</sub> OH Conversion. ChemCatChem, 2019, 11, 621-627.	3.7	29
53	Finding the active species: The conversion of methanol to aromatics over Zn-ZSM-5/alumina shaped catalysts. Journal of Catalysis, 2021, 394, 416-428.	6.2	29
54	Structure, activity and kinetics of supported molybdenum oxide and mixed molybdenum–vanadium oxide catalysts prepared by flame spray pyrolysis for propane OHD. Applied Catalysis A: General, 2014, 472, 29-38.	4.3	27

#	Article	IF	CITATIONS
55	<i>Operando</i> XAS/XRD and Raman Spectroscopic Study of Structural Changes of the Iron Molybdate Catalyst during Selective Oxidation of Methanol. ChemCatChem, 2019, 11, 4871-4883.	3.7	26
56	The impact of reaction conditions and material composition on the stepwise methane to methanol conversion over Cu-MOR: An operando XAS study. Catalysis Today, 2019, 336, 99-108.	4.4	26
57	Electronic and Geometrical Structure of Zn <sup>+</sup> Ions Stabilized in the Porous Structure of Zn-Loaded Zeolite H-ZSM-5: A Multifrequency CW and Pulse EPR Study. Journal of Physical Chemistry C, 2017, 121, 14238-14245.	3.1	25
58	Hierarchical ZSM-5 prepared by guanidinium base treatment: Understanding microstructural characteristics and impact on MTG and NH3-SCR catalytic reactions. Catalysis Today, 2011, 168, 71-79.	4.4	24
59	Systematic study on the influence of the morphology of α-MoO3 in the selective oxidation of propylene. Journal of Solid State Chemistry, 2015, 228, 42-52.	2.9	24
60	Tuning the material and catalytic properties of SUZ-4 zeolites for the conversion of methanol or methane. Microporous and Mesoporous Materials, 2018, 265, 112-122.	4.4	24
61	Single-Event MicroKinetics (SEMK) for Methanol to Hydrocarbons (MTH) on H-ZSM-23. Catalysis Today, 2013, 215, 224-232.	4.4	23
62	Influence of post-synthetic modifications on the composition, acidity and textural properties of ZSM-22 zeolite. Catalysis Today, 2018, 299, 120-134.	4.4	23
63	Catalytic hydropyrolysis of biomass using supported CoMo catalysts – Effect of metal loading and support acidity. Fuel, 2020, 264, 116807.	6.4	22
64	Impact of post-synthetic treatments on unidirectional H-ZSM-22 zeolite catalyst: Towards improved clean MTG catalytic process. Catalysis Today, 2018, 299, 135-145.	4.4	21
65	Co-conversion of methanol and light alkenes over acidic zeolite catalyst H-ZSM-22: Simulated recycle of non-gasoline range products. Applied Catalysis A: General, 2015, 494, 68-76.	4.3	19
66	From Colloidal Monodisperse Nickel Nanoparticles to Well-Defined Ni/Al <sub>2</sub> O <sub>3</sub> Model Catalysts. Langmuir, 2017, 33, 9836-9843.	3.5	19
67	Identification of Distinct Framework Aluminum Sites in Zeolite ZSM-23: A Combined Computational and Experimental <sup>27</sup> Al NMR Study. Journal of Physical Chemistry C, 2019, 123, 7831-7844.	3.1	19
68	Exploring Scaling Relations for Chemisorption Energies on Transitionâ€Metalâ€Exchanged Zeolites ZSMâ€22 and ZSMâ€5. ChemCatChem, 2016, 8, 767-772.	3.7	18
69	Zeolite morphology and catalyst performance: conversion of methanol to hydrocarbons over offretite. Catalysis Science and Technology, 2017, 7, 5435-5447.	4.1	18
70	Topology-dependent hydrocarbon transformations in the methanol-to-hydrocarbons reaction studied by <i>operando</i> UV-Raman spectroscopy. Physical Chemistry Chemical Physics, 2018, 20, 26580-26590.	2.8	18
71	Temperature-programmed reduction with NO as a characterization of active Cu in Cu-CHA catalysts for NH <sub>3</sub> -SCR. Catalysis Science and Technology, 2019, 9, 2608-2619.	4.1	17
72	Methanol Conversion to Hydrocarbons (MTH) Over H-ITQ-13 (ITH) Zeolite. Topics in Catalysis, 2014, 57, 143-158.	2.8	16

#	Article	IF	CITATIONS
73	Operando UV-Raman study of the methanol to olefins reaction over SAPO-34: Spatiotemporal evolution monitored by different reactor approaches. Catalysis Today, 2019, 336, 203-209.	4.4	16
74	Comparing the Nature of Active Sites in Cu-loaded SAPO-34 and SSZ-13 for the Direct Conversion of Methane to Methanol. Catalysts, 2020, 10, 191.	3.5	16
75	Alkali Earth Metal Molybdates as Catalysts for the Selective Oxidation of Methanol to Formaldehyde—Selectivity, Activity, and Stability. Catalysts, 2020, 10, 82.	3.5	15
76	Enhanced Catalytic Performance of Zn ontaining HZSMâ€5 upon Selective Desilication in Ethane Dehydroaromatization Process. ChemCatChem, 2020, 12, 1519-1526.	3.7	14
77	Influence of Cu-speciation in mordenite on direct methane to methanol conversion: Multi-Technique characterization and comparison with NH3 selective catalytic reduction of NOx. Catalysis Today, 2021, 369, 105-111.	4.4	14
78	Mapping the coke formation within a zeolite catalyst extrudate in space and time by operando computed X-ray diffraction tomography. Journal of Catalysis, 2021, 401, 1-6.	6.2	14
79	Stability of Iron-Molybdate Catalysts for Selective Oxidation of Methanol to Formaldehyde: Influence of Preparation Method. Catalysis Letters, 2020, 150, 1434-1444.	2.6	13
80	Deactivation of a CoMo Catalyst during Catalytic Hydropyrolysis of Biomass. Part 1. Product Distribution and Composition. Energy & amp; Fuels, 2019, 33, 12374-12386.	5.1	11
81	Deactivation of a CoMo Catalyst during Catalytic Hydropyrolysis of Biomass. Part 2. Characterization of the Spent Catalysts and Char. Energy & Fuels, 2019, 33, 12387-12402.	5.1	10
82	Hierarchical Vanadia Model Catalysts for Ammonia Selective Catalytic Reduction. Topics in Catalysis, 2017, 60, 1631-1640.	2.8	9
83	Cu-Exchanged Ferrierite Zeolite for the Direct CH4 to CH3OH Conversion: Insights on Cu Speciation from X-Ray Absorption Spectroscopy. Topics in Catalysis, 2019, 62, 712-723.	2.8	9
84	Synthesis of ZSM-23 (MTT) zeolites with different crystal morphology and intergrowths: effects on the catalytic performance in the conversion of methanol to hydrocarbons. Catalysis Science and Technology, 2019, 9, 6782-6792.	4.1	7
85	Vanadia-Based Catalysts for the Sulfur Dioxide Oxidation Studied <i>In Situ</i> by Transmission Electron Microscopy and Raman Spectroscopy. Journal of Physical Chemistry C, 2017, 121, 3350-3364.	3.1	6
86	The role of platinum on the NO <sub>x</sub> storage and desorption behavior of ceria: an online FT-IR study combined with <i>in situ</i> Raman and UV-vis spectroscopy. Physical Chemistry Chemical Physics, 2021, 23, 1874-1887.	2.8	6
87	From Catalytic Test Reaction to Modern Chemical Descriptors in Zeolite Catalysis Research. Chemie-Ingenieur-Technik, 2021, 93, 902-915.	0.8	5
88	Atomic-scale Dynamics in Catalysts for Sulfur Chemistry. Microscopy and Microanalysis, 2015, 21, 421-422.	0.4	0